

DYNAMIC BENCHMARKING OF TREMOLO -- A PROGRAM FOR PIPELINE TWO-PHASE FLOW TRANSIENT ANALYSIS

**G. Thomas Elicson, Robert E. Henry,
Robert J. Hammersley, and James P. Burelbach**
Fauske & Associates, Inc.
16W070 West 83rd Street
Burr Ridge, IL 60512
henry@fauske.com burelbach@fauske.com

KEY WORDS

Transient, Thermal-hydraulics, Two-phase, Pipeline, TREMOLO

ABSTRACT

The TREMOLO computer program has been used to analyze two-phase flow transients in service water piping systems in nuclear power plants in response to NRC Generic Letter 96-06 (USNRC, 1996). These analyses have been concerned with two-phase flow heat transfer in containment fan coolers and waterhammer events resulting from steam condensation and water column rejoining. To support these applications, the TREMOLO code has been validated with benchmarks against available data. TREMOLO utilizes a “dynamic benchmarking” feature first introduced by Henry (1996a, 1996b, 1997a, 1997b) and Paik (1996) whereby a set of dynamic benchmarks is embedded in the source code and is exercised every time the archived code is updated. Thus, the purpose of this paper is two-fold: to present the concept of dynamic benchmarking as implemented in TREMOLO and to provide benchmark results used to validate the TREMOLO code for nuclear power plant applications related to Generic Letter 96-06. Insights gained during the benchmarking effort related to key phenomena and relevant computer models are also provided in the discussion of benchmark results.

1. INTRODUCTION

Currently, in the nuclear industry, issues related to condensation-induced waterhammer events in the service water piping of containment air coolers are being addressed in response to NRC Generic Letter 96-06 (USNRC, 1996). The issue of concern in the air cooler systems of nuclear power plants is whether the hydrodynamic loads imposed by waterhammer events could be large enough to challenge the integrity of safety-related service water piping. For example, during a postulated loss of power event, due to the stoppage of the service water pump, the piping in an open cooling water system for the containment air coolers, initially filled with cold, single-phase flowing liquid, would experience a transient drain down. Typically, piping high points exist on both the air cooler supply and return piping, thus the transient drain down could lead to column separation in both the supply and return piping.

If a loss of coolant accident (LOCA) in containment is postulated to occur coincident with the loss of power, then the heat input to the cooling water combined with the lower service water flow rate would lead to steam generation and voiding of the air cooler and attached piping. The void progression into the attached and initially cold supply and return piping would displace water from that piping.

Steam condensation would occur on the exposed, cold piping and influence the extent of the void progression. Upon restoration of electrical power (due to startup of an emergency diesel generator) and the return of the service water pump capacity (typically assumed to occur within 40 seconds of the loss of power event), the voided regions of the service water piping as well as the containment air cooler would be refilled. Given the preceding scenario it is likely that multiple condensation-induced waterhammer events would occur both during the initial voiding phase as well as during the refill phase. These dynamic events have been observed experimentally (Henry, 1999, Hammersley, 1999).

Although fluid flow transients in thermal power plant piping systems have received considerable attention over the past several decades (USNRC, 1979; Serkiz, 1984; Izenon, 1988), including the consideration of condensation-induced waterhammer events in cooling water systems (Safwat, 1972, Henry, 1999), the challenges inherent in developing analytical tools suitable for application to the loss of power and LOCA scenario discussed above remain. Consider, for instance, the issues of scale that complicate real plant applications. Typically, the air cooler supply and return piping may consist of several hundred meters of piping with several changes in pipe diameter and upwards of 100 different elbows, tees, expansions, and valves. In contrast, the dynamic loads of interest may occur in only a few tens of centimeters of the 100+ meter pipe circuit and affect only a handful of the piping flow elements. Also, while the transient of interest unfolds over 60 seconds, or more, the dynamic effects occur on a millisecond time scale.

The TREMOLO computer code has been developed and applied to the issues of condensation-induced waterhammer in power plant cooling systems discussed above. A series of code benchmarks has been performed using a “dynamic benchmarking” process. The outcome of these benchmarks will ultimately demonstrate whether the TREMOLO methodology is applicable to the analysis of two-phase flow and condensation-induced waterhammer events that are postulated to occur in the service water piping systems of nuclear power plants. The purpose of this paper is, therefore, to discuss the dynamic benchmarking process implemented in TREMOLO and present results of the benchmarking activities.

2. APPROACH TO DYNAMIC BENCHMARKING AND INTEGRATION INTO THE TREMOLO CODE

Very often, in the course of integrated code development, the various phenomena and analytical models incorporated into the integrated code have been tested, benchmarked, and validated. After the development phase of such codes has finished, releasing it to the production/maintenance phase, the previous tests and benchmarks may not necessarily be repeated for new code versions or revisions of the code as additional capabilities are added, errors are corrected, etc. Therefore, for such codes, it is important to integrate the benchmarking/validation tests into the code so that as the code gets upgraded, the benchmarks and validation tests can be easily repeated and can be repeated by anyone including developers and end users. Through this process, the developers and users can continually examine the benchmark and validation tests as the code evolves to assure that the code’s predictive capabilities are maintained. The concept outlined above is referred to as dynamic benchmarking since the benchmarking and validation tests can be easily repeated for any code version at any point of time in the code’s history (Henry 1996a, 1996b, 1997a, 1997b and Paik, 1996).

From a code development point of view, the dynamic benchmarking concept involves embedding benchmark instructions within the source code such that the “off the shelf” code can be exercised every time the archived code is updated. Thus, the dynamic benchmarks enable the testing of individual code models and subroutines in the exact form in which the models and subroutines are implemented in the archived code. Furthermore, embedding benchmark instructions and relevant experimental data within the code provides a permanent record of the benchmark information. This is in contrast to the classic approach of extracting desired subroutines and writing standalone driver modules

to perform the testing.

2.1 Summary of TREMOLO Dynamic Benchmarks

In TREMOLO, the dynamic benchmarking capability is integrated into the source code and falls into two categories: separate effects tests and integral experiment benchmarks. The separate effects tests exercise individual physics modules to demonstrate that key phenomena are adequately modeled by the code. The integral experiment benchmarks exercise the entire code to demonstrate the overall code applicability to applied problems in transient two-phase pipe flow. Table 1 provides a summary of the TREMOLO dynamic benchmarking capability. Note that additional benchmarks have been performed using the classic benchmark approach and have yet to be integrated into the TREMOLO source code. Work continues to incorporate additional benchmarks such that over time the data base of dynamic benchmarks continues to grow.

2.2 Computer Code Structure to Support Dynamic Benchmarking

The benchmark results that are presented in Section 4 focus on integral experiment benchmarks related to transient flow problems similar to those postulated to occur in the service water systems of nuclear power plants. These benchmarks are controlled through the use of an executive subroutine, BENCH, which in turn calls the specific benchmark subroutines based on user input specifications. The names of the specific benchmark routines are provided in Table 1.

Table 1 Summary of Available TREMOLO Dynamic Benchmarks.

Benchmark Description	Benchmark Type	Benchmark Driver Subroutine Name
Containment air cooler heat exchanger model benchmarked against steady state vendor tests over a range of gas and cooling water temperatures and flow rates	Separate effect	BQFANCL
Two-phase sonic velocity model benchmarked against experimental measurements for void from 0 to 50%	Separate effect	BSONVEL
Calculation of pressure drop with low quality, high velocity flashing flows benchmarked against experimental measurements	Separate effect	BDELPUP
Reynolds Number-dependent smooth pipe friction factor model benchmarked against handbook values	Separate effect	BFFACTR
Model for reaction force in a pipe bend compared against a textbook analytical solution	Separate effect	BFBEND
Model for reaction force in a 90-degree elbow compared against a textbook analytical solution	Separate effect	BXFORCE
Delft Hydraulics Laboratory Pressure Surge Test 180: cold water column separation and rejoining in a prototypic condenser piping system	Integral experiment	BDELFT180
Simulation of all liquid waterhammer in a	Integral experiment	BLIQHAMMER

municipal water system		
Two-phase waterhammer experiment caused by sudden closure of a motor-operated valve	Integral experiment	BMOV
FAI Test 49 simulating voiding and refill of fan cooler piping	Integral experiment	BFAI49

The individual benchmark subroutines contain information on the experimental initial and boundary conditions such as the timing, duration, and strength of any source flows. In some instances the benchmark subroutines also execute instructions for analytical solutions or bounding estimates of the test at hand or include instructions for running third party graphics software to automatically generate comparison plots of the code calculations and the experimental data. Also, for separate effects tests, the dynamic benchmark routines can allow tests to be performed over a range of sensitivity parameters. In general, since the experiment data files are quite large, they are not imbedded in the source code, and therefore must be stored in a controlled computer archive alongside of the archived computer code source files.

Input requirements to execute the dynamic benchmarks are similar to those required to perform a plant analysis calculation. Namely, a “parameter file” must be supplied which contains details of the system geometry, code modeling parameters, initial and boundary conditions, and pipe nodalization. In addition, a sequence-specific input file must be provided which makes any sequence-specific changes to inputs provided in the base parameter file and sets up the program time control or restart functions. The parameter file typically contains several hundred separate pieces of input to describe the system being modeled, therefore a unique parameter file must be developed for each benchmark and stored in the computer archive. A one line specification in a sequence input file is all that is then required to activate the dynamic benchmark routines for a specific test. If a separate effect test is specified via input, then the benchmark routines access only those routines necessary to perform the individual model calculations. If an integrated experiment benchmark is selected, then the benchmark routines control certain initial and boundary conditions but otherwise allow normal execution of the entire, integrated code.

3. TREMOLO CODE DESCRIPTION

TREMOLO is a transient thermal hydraulic code developed to analyze single- and two-phase flow conditions in plant piping systems. TREMOLO – **T**hermal hydraulic **R**esponse of a **M**otor-**O**perated valve **L**ine – was so named since it was originally developed in response to NRC Generic Letter 89-10 (USNRC, 1989) to evaluate pressure oscillations associated with valve closures and openings in piping segments that could be exposed to two-phase flow conditions. Incidentally, a rapid fluctuation of a musical tone caused by the reiteration of pressure waves is also known as a tremolo.

The TREMOLO code contains models of the phenomena relevant to the study of transient two-phase flow and condensation-induced waterhammer events that could occur in process piping systems. These models were selected and developed based on an understanding of the dominant physical processes expected during accident conditions postulated to occur in service water cooling systems of nuclear power plants. Namely, based on in-house scaled experiments, and a review of the open literature, the dominant phenomena modeled in TREMOLO include, one-dimensional, non-equilibrium, two-phase fluid flow; presence and influence of residual gas bubbles in the fluid following large scale void collapse; steam condensation on cold pipe walls; steam condensation on the cold liquid phase; non-condensable gas coming out of solution at pressures higher than the saturation pressure corresponding to the liquid temperature; and fan coil heat transfer. Each of these models is briefly discussed, below.

3.1 One-Dimensional Fluid Conservation Equations

TREMOLO is a node and junction code that uses a one-dimensional, “one and a half” fluid model which implies separate mass and energy equations for each of the two fluid phases and a single momentum equation to describe the fluid mixture. TREMOLO considers two fluid phases (liquid and vapor), which may exist in a non-equilibrium state. To provide closure to this system of equations, fluid transport between the phases is defined and an equation of state is used.

3.2 Equation of State

The TREMOLO equation of state determines the fluid temperature and pressure in a fluid node given the total mass and energy of each fluid phase in the node. Given the total mass and energy, the fluid mixture sonic velocity and density are calculated. Then, for all-liquid and low void mixtures, the node pressure is computed based on the fluid compressibility, as,

$$P = P_{sat} + a_w^2 \cdot (\rho_{fluid} - \rho_{sat}) \quad (1)$$

In this equation, the saturation properties are evaluated at the liquid phase temperature.

If the gas phase compressibility controls the pressure in a fluid node (i.e., for nodes with high void fractions), the fluid phases are assumed to be separated and to exist at equal pressures. In this instance, the ideal gas law is applied to the gas phase, Eq. (1) is applied to the liquid phase, and a gas phase energy balance is performed. These three equations are then solved simultaneously to determine the node pressure, the gas temperature, and the gas volume.

For postulated accidents in which boiling in the service water piping may occur, or subatmospheric conditions may be obtained, noncondensable gasses could be expected to come out of solution. If subsequent conditions cause the steam to be condensed, the noncondensable gases would affect both the steam condensation and the water compressibility. Of particular note is that the air cannot be driven back into solution as efficiently as it exits solution during the initial vaporization process. Therefore, after the larger scale steam condensation takes place, a significant second phase would still exist and would be the composite of the remaining noncondensable gases and the steam existing at the partial pressure equal to the water temperature at the gas bubble-water interface. As a result, the “cushioning” of this far more compressible fluid reduces the waterhammer pressures caused by the condensation process.

To account for the residual gas volume that may exist after larger scale condensation, the TREMOLO equation of state retains a minimum void fraction in a particular node which is equal to the maximum void calculated in the node up to a user-specified residual void fraction limit. The residual void is then used when calculating the fluid sonic velocity for use in Eq. (1), above. The dynamic benchmarks presented in Sections 4.2 (for warm water) and Section 4.3 (for cold water in a closed condenser cooling water system) validate this modeling approach and conclude that residual void limits in the range of .0005 to .005 produce the best comparison with the test data.

3.3 Phase Interface Model

The transport of mass and energy between the phases is based on the growth of noncondensable and steam bubbles in a very low void fraction regime. Under these conditions, the model assumes that the steam bubble growth is thermally dominated such that it is controlled by conduction across the thermal boundary layer in the superheated water (Tong, 1965). The driving force for heat transfer is,

then, the temperature difference between the liquid phase and the saturation temperature at the steam partial pressure in the bubble. Also, the heat transfer surface area is based on the total bubble surface area. The model requires user-specified model parameters to describe the initial bubble radius, the number of bubbles per unit volume, and the initial non-condensable gas partial pressure. The model then calculates the rate of change of the steam mass and energy, as well as the change in the bubble radii (and hence the phase interface heat transfer surface area).

3.4 External Heat Sources and Sinks

Energy gain and loss may occur across pipe walls and within heat exchanger cooling coils. The pipe walls are treated as one-dimensional heat sinks in the radial direction, with several options for pipe wall boundary conditions.

The TREMOLO geometry model allows users to build a complete pipe circuit by developing and assembling individual pipe sections according to the way in which pipe sections appear on piping isometrics. Once the pipe sections are defined, the pipe wall boundary conditions can be assigned for each pipe section individually. The inside surface of the pipe may be treated with an adiabatic, convective, or constant heat flux boundary. If a convective boundary condition is selected, then the Reynolds-Colburn analogy (Holman, 1981) is used to determine the heat transfer coefficient for all liquid flow,

$$h = \frac{f}{8} \cdot \rho \cdot c_p \cdot u_\infty \quad (2)$$

For two-phase flows, the flow pattern is treated as either annular or plug flow. The annular flow model assumes that only the liquid phase is in contact with the pipe wall, therefore only the liquid phase transfers heat directly with the pipe wall. The vapor phase energy balance is indirectly affected as it must transfer heat to the liquid phase, as discussed in Section 3.3. The plug flow model assumes both phases contact the pipe wall in proportion to their volume fractions. The liquid phase heat transfer coefficient is then calculated according to Eq. (2), above, while a constant condensation heat transfer coefficient is assumed for the vapor phase. For the constant heat flux boundary condition, a heat flux may be specified separately for each individual pipe section, as defined through user input.

The pipe outside surface boundary condition may be specified as either adiabatic or convective. For a convective boundary, the bulk gas temperature and heat transfer coefficient are specified by the user for each pipe section. Since pipe circuits may consist of several hundred meters of pipe, this approach allows the varying conditions on the outside of the pipe to be appropriately modeled.

Finally, a pipe section may be defined as heat exchanger, in which case heat transfer is based on either a mechanistic heat exchanger model or a lookup table consisting of pairs of cooling water flow rates and corresponding heat transfer rates. The mechanistic heat exchanger model accounts for low flow and two-phase flow conditions in the cooling water and time-dependent gas temperatures on the outside of the heat exchanger.

3.5 Code Numerics

The rate equations discussed in Section 3.1 are expressed as difference equations using an upwind differencing scheme, then integrated in time with a classic 4th order Runge-Kutta integration scheme coupled with a variable time step.

Use of an explicit integration scheme leads to sometimes large numerical errors during rapid

fluid transients unless a time step is selected much smaller than the maximum allowed by the Courant condition,

$$Dt_{\max} = \frac{Dx}{a_w} \quad (3)$$

Typically, the actual time step would have to be an order of magnitude smaller than Δt_{\max} . Thus, an “anticipatory” term is added to the momentum rate equation to limit the change in momentum during rapid changes in pressure or fluid density, such as would occur as a pressure wave or a void-liquid interface travels through the fluid node. The anticipatory term uses a centered-space difference formulation which goes to zero during steady state conditions and increases in magnitude as the conditions in adjacent nodes diverge:

$$\frac{dw_i}{dt} = \frac{dw_i}{dt} + K \cdot (w_{i-1} - 2 \cdot w_i + w_{i+1}) \quad (4)$$

As shown in Eq. (4), a linear multiplier, K, referred to here as a “numerical damping factor” is included to control the fidelity of the anticipatory term. The advantage of the anticipatory term of Eq. (4) is that the explicit integration scheme can be used with minimal numerical error while taking time steps close to the maximum allowed by the Courant condition. The downside is that an excessively large damping factor can noticeably distort the pressure wave propagation speed. Sensitivity studies indicate that a numerical damping factor in the range of 10 to 80 provides reasonable gains in numerical accuracy while minimizing distortions to the wave speed. The impact of the anticipatory approach can be seen in the results of the all liquid waterhammer benchmark exercise, presented in Section 4.1.

4. RESULTS OF INTEGRAL CODE BENCHMARKS

The following integral experiment benchmarks focus on transient flow problems similar to those postulated to occur in the service water systems of nuclear power plants resulting from a loss of offsite power. TREMOLO dynamic benchmarks against experimental data simulating a loss of coolant accident (LOCA) coincident with a loss of offsite power can be found in Hammersley, et al. (1999). Analyses of these types of transient flow problems are motivated by the need for the nuclear industry to respond to NRC Generic Letter 96-06 (USNRC, 1996).

4.1 All Liquid Waterhammer Benchmark Against Method of Characteristics Solution

A sample run was performed with TREMOLO to simulate an all liquid waterhammer event in a municipal water system. Results of the TREMOLO analysis are then compared against a method of characteristics (MOC) solution described in Wylie and Streeter (1978). The purpose of this benchmark is to demonstrate the capability of TREMOLO to calculate rapid waterhammer pressure rises, therefore use of an all liquid system provides a limiting analysis in terms of the pressure wave transmission speed and pressure rise time. Since this benchmark is free of any steam-liquid phase transition phenomena, results of the benchmark will present a clear picture of the magnitude of numerical errors present in the explicit integration scheme employed in TREMOLO and the impact of the anticipatory technique defined in Eq. (4), above.

Details of the all liquid waterhammer benchmark include: total pipe length: 932.7 m (3060 ft); pipe elevation change from inlet to outlet: 0 m (0 ft); constant pipe inside diameter: 0.076 m (0.25 ft);

constant upstream reservoir pressure: 1.02 MPa (148 psia); initial steady state flow through the pipe: 0.332 m/s (1.09 ft/s); and total pressure drop during steady state conditions: 0.020 MPa (2.9 psi).

Steady state conditions are assumed initially, then a valve located at the end of the pipe is closed instantaneously, giving rise to the waterhammer event as the water column velocity is reduced by the closed valve. The high pressure wave originating at the closed valve will travel to the upstream reservoir which is held at a constant pressure and a pressure wave will be reflected back toward the closed valve. Because of the large pipe length, instantaneous valve closure, and all liquid conditions, the peak pressure rise observed at the valve face will approach the theoretical maximum pressure calculated from the Joukowsky equation,

$$DP = \rho u a_w \quad (5)$$

Given a sonic velocity of 1439 m/sec (4722 ft/s) based on water density and bulk modulus at 302 K (85° F) and an initial water velocity of 0.332 m/s (1.09 ft/sec) at a density of 998 kg/m³ (62.4 lbm/ft³), the Joukowsky equation yields a pressure rise of 0.477 MPa (69.2 psi).

Results of the TREMOLO calculations are presented in Figure 1. Also shown in the figure are calculations based on a method of characteristics (MOC). While the ideal wave shape approaches that of a square wave, the TREMOLO pressure calculation overshoots the peak pressures shown in the MOC solution then dampens out as the numerical error diminishes. The resulting TREMOLO pressure then closely follows the MOC calculation. Furthermore, the initial pressure rise at the valve location in both the MOC and TREMOLO calculation match the theoretical peak pressure calculated from Eq. (5). To overcome the numerical error inherent in the TREMOLO explicit integration scheme, the numerical damping multiplier defined in Eq. (4), above, was set to 10. Figure 1 indicates that this level of damping has a minimal impact on the pressure wave propagation speed while reducing the numerical error to acceptably low levels. Also, through use of the numerical damping, a time step equal to the maximum allowed by the Courant condition was used.

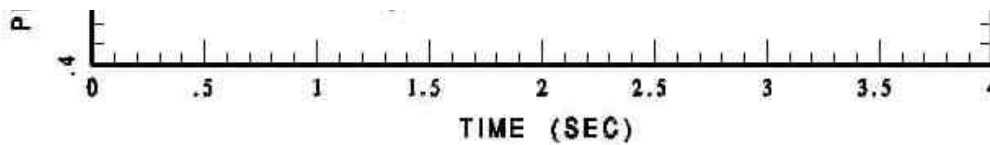


Figure 1 Results of all liquid waterhammer benchmark for a pipe length of 932.7 m, initial reservoir pressure of 1.02 MPa, initial fluid velocity of 0.332 m/sec, fluid density of 998 kg/m³, and sonic velocity of 1439 m/sec.

4.2 MOV Test: Condensation-Induced Waterhammer Due to Sudden Valve Closure

This benchmark focuses on condensation-induced waterhammer under low void conditions. The two-phase conditions are obtained experimentally by first establishing steady state flow of slightly subcooled water through a pipe, then suddenly closing a valve at the end of the pipe. The pressure response at the valve gate face is controlled first by an all-liquid waterhammer event as the closed valve suddenly stops the flowing fluid. Once the resulting high-pressure wave propagates to the upstream reservoir and returns (with a magnitude now based on the upstream reservoir pressure) to the closed valve, a rarefaction wave, originating at the valve disk, then travels upstream. Due to the elevated fluid temperature, the rarefaction wave is limited to the fluid saturation temperature, and, as the low-pressure wave travels upstream, steam voids are formed behind the wave. Once again a pressure wave reflects off the upstream reservoir and begins to propagate toward the closed valve. This time, however, the pressure wave is traveling through a two-phase, bubbly fluid characteristic of flowing fluids with low steam void fractions. As the returning pressure wave moves down the pipe, steam voids begin to collapse, until, finally, the pressure wave reaches the closed valve whereupon a condensation-induced waterhammer event is observed. This condensation-induced waterhammer event is most closely characterized by the trapped void collapse classification of waterhammer events described in NUREG/CR-5220, Vol. 1 (Izenson, 1988).

This benchmark is relevant to the Generic Letter 96-06 analyses because its outcome is dependent on the ability of TREMOLO to properly model several key phenomena expected to exist in the Generic Letter 96-06-type transients. For instance, the benchmark provides a test of the models for pressure wave propagation through a combined single and two-phase fluid mixture, the ability of the phase interface transport model to generate and condense steam in non-equilibrium fashion, and the applicability of the one-dimensional, five-equation fluid model incorporated into TREMOLO to model this type of waterhammer event. Furthermore, this benchmark validates the empirical approach used in TREMOLO of retaining a minimum residual void in a fluid node following the larger scale void collapse, as described in Section 3.2, above.

Results of this column separation benchmark, presented in Figure 2, compare the experimental data, RELAP5/MOD 3.2, and method of characteristics transient calculations reported by Cerne (1996) against TREMOLO calculations. Key features of the experiment include a large reservoir containing water at 436 K (325 F), connected to a 36 m (120 ft) pipe with a nominal pressure of 1 MPa (145 psia), and an initial fluid velocity through the pipe of 0.4 m/sec (1.3 ft/sec). A valve at the end of the pipeline is closed instantaneously and the ensuing pressure transient near the valve inlet is shown in Figure 2. The TREMOLO code calculations closely follow the timing, shape, and magnitude of the experimentally observed pressure transient, indicating that the important phenomena of pressure wave propagation through single and two-phase mixtures, flashing, and steam condensation are appropriately modeled. The pressure transient calculated by TREMOLO occurs slightly earlier than that observed in

the test data, indicating that the pressure wave propagation speed in TREMOLO is slightly higher than the actual wave speed. Since the maximum void size calculated by TREMOLO is on the order of 0.1%, the calculations are sensitive to uncertainties in the steam void and the resulting effect on sonic velocity.

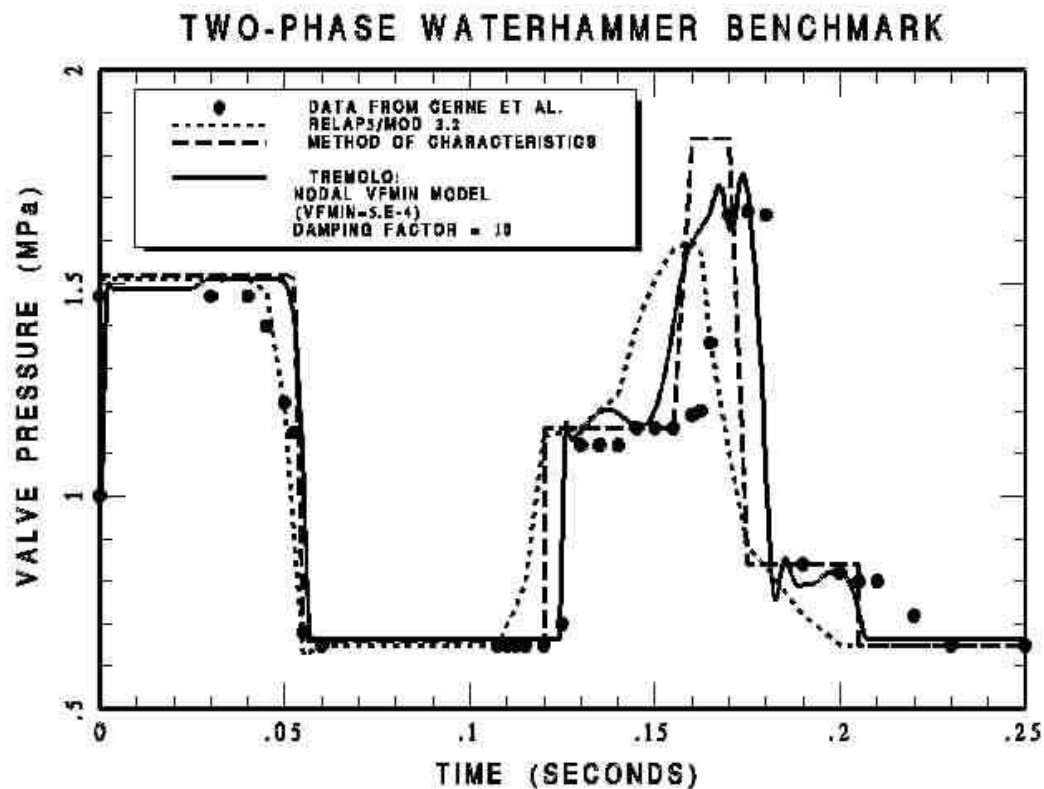


Figure 2 Two-phase waterhammer benchmark for initial conditions of 1 MPa nominal pressure, 436 K fluid temperature, and 0.4 m/sec liquid velocity with sudden valve closure 36 m downstream at time zero. TREMOLO empirical parameter settings include residual void fraction of .0005 and numerical damping factor of 10.

4.3 Delft Hydraulics Laboratory Test 180: Pressure Surges in Condenser Cooling Water Systems

The experimental investigations of Safwat (1972) at the Delft Hydraulics Laboratory provide insight into the effects of cold water column separation and rejoining in piping systems that are prototypic of those used in condenser cooling water systems of thermal power plants. The investigations of Safwat focus on the transient flow events that could occur as the result of a power failure and subsequent loss of the cooling water system pump. Safwat reports that if the condenser is

located in an elevated portion of the cooling water system, relative to the pump discharge centerline, then a pump trip would initially result in column separation in the elevated portion of the piping. This occurs as the momentum of the water column results in continued forward flow of the water through the condenser return piping while at the same time gravity effects cause a flow reversal in the riser of the condenser supply piping. Furthermore, since Safwat simulated pump trip by closing a ball valve near the piping system inlet, a column separation was also observed in the piping near the closed valve. Thus, the growth and collapse of two separate steam void regions and the movement of two separate water columns characterize the experiments of Safwat. This geometry is qualitatively shown in Figure 3.

The pressure surge experiments of Safwat lead to three general types of waterhammer events. First, near the closed ball valve, there is the trapped void collapse, similar to that described in NUREG/CR-5220, Vol. 1 (Izenson, 1988). This occurs as water column 1 in Figure 3 reverses direction, collapses steam void 1, and contacts the closed ball valve. Second, there is a trapped void collapse as the two separate water columns rejoin in the elevated portion of the piping system. In some instances one water column may be essentially stagnant while the other water column moving with some velocity compresses the voided region (void 2 in Figure 3) and impacts the stagnant column. In other instances, both water columns may be moving toward each other with independent velocities prior to the column rejoining. The third type of waterhammer event is the classic, all liquid waterhammer which could result when water columns 1 and 2 rejoin while column 1 is in complete contact with the closed valve. The pressure wave originating at the point of the column rejoining event would be transmitted along the length of water column 1 and impact the closed valve.

This benchmark is relevant to the Generic Letter 96-06 analyses because it models cold water column separation and rejoining events that could occur in the service water systems of nuclear power plants following a loss of offsite power without a LOCA. Furthermore, the test apparatus used in the pressure surge tests contains an elevated condenser section that is typical of the condenser cooling water systems found in nuclear power plants. This benchmark will exercise the TREMOLO capabilities for modeling of flow reversal, draindown from an elevated piping section, the growth and collapse of multiple voided regions, the behavior of two independent water columns, and the condensation-induced water hammer events that occur due to column rejoining and trapped void collapse.

This benchmark focuses specifically on pressure surge Test 180. Details of this test are as follows. The test apparatus, depicted in Figure 3, consists of a high-level water reservoir connected to a 18.7 m horizontal run of 0.09 m inner diameter piping. The ball valve used to simulate pump trip is located near the inlet of the horizontal piping run. Next, a 5.6 m vertical riser leads to the simulated condenser section. The condenser consists of cylindrical inlet and outlet headers (0.2 m diameter) interconnected by 12 condenser tubes of 0.02 m inner diameter and 2 m length, running in parallel to each other. The outlet header is then connected through a 90-degree elbow to the return downcomer, which runs vertically downward to a 18.7 m long horizontal return pipe. The horizontal runs of supply and return pipe are at the same elevation. The horizontal return pipe discharges into a low-level water reservoir. The initial water temperature is 293 K, the steady state flow yields a velocity of 1.11 m/s, the high-level reservoir pressure is 0.1185 MPa and the total pressure drop through the system at steady state conditions is 0.0169 MPa. To initiate the transient, the ball valve begins closing at 0.158 seconds and is fully closed at 1.158 seconds.

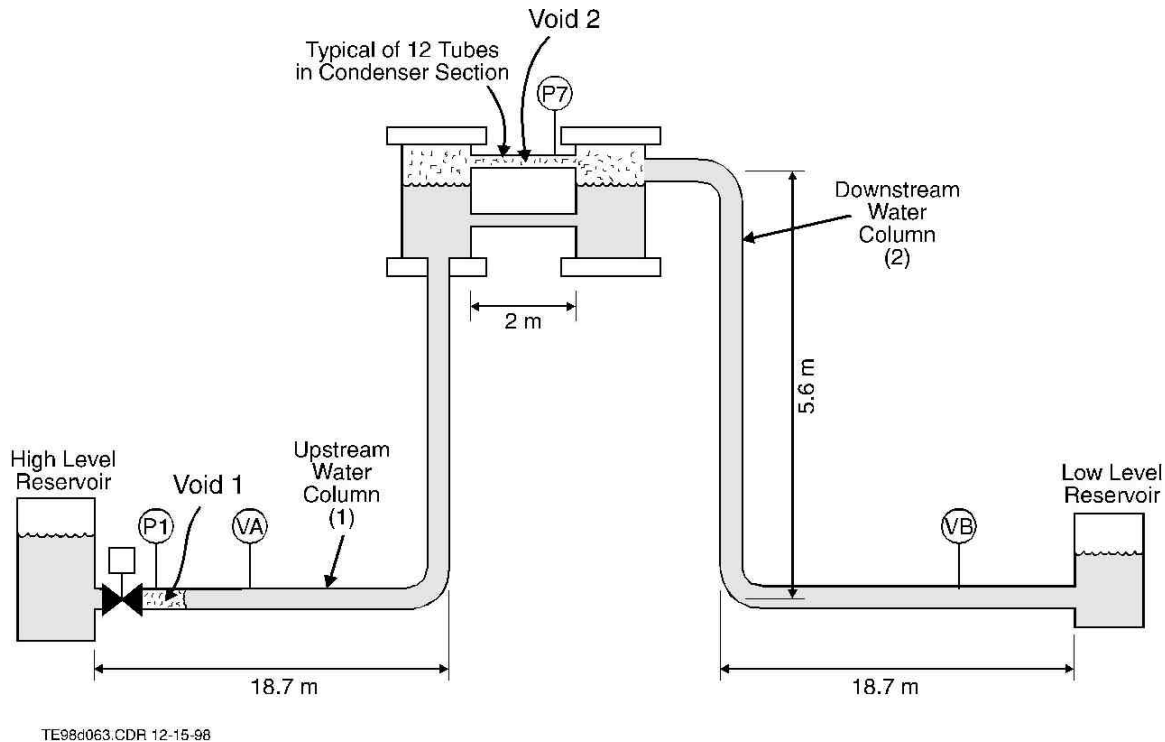


Figure 3 Delft Hydraulics Laboratory test configuration for pressure surge test 180 with a depiction of the separate voided regions and water columns following column separation. Based on Safwat (1972).

Note that the test apparatus is a closed piping system. Upon completion of each test run, water was pumped from the low-level reservoir back to the high-level reservoir and any non-condensable gas accumulating in the condenser highpoints was reportedly vented prior to initiation of the next test run. Thus, the non-condensable gas content in the subcooled water is likely less than that expected in the open service water system found in many nuclear power plants. A key feature of the TREMOLO model is the treatment of residual gas bubbles in the fluid following void collapse. Following column rejoining, this small residual void will have an effect on pressure wave propagation speeds and subsequent waterhammer events. The residual void volume used in TREMOLO is an assumed value based on experimental evidence. Therefore, the appropriate value of the residual void for the closed cooling water circuit used for pressure surge test 180 will not be typical of that used for open cooling water system.

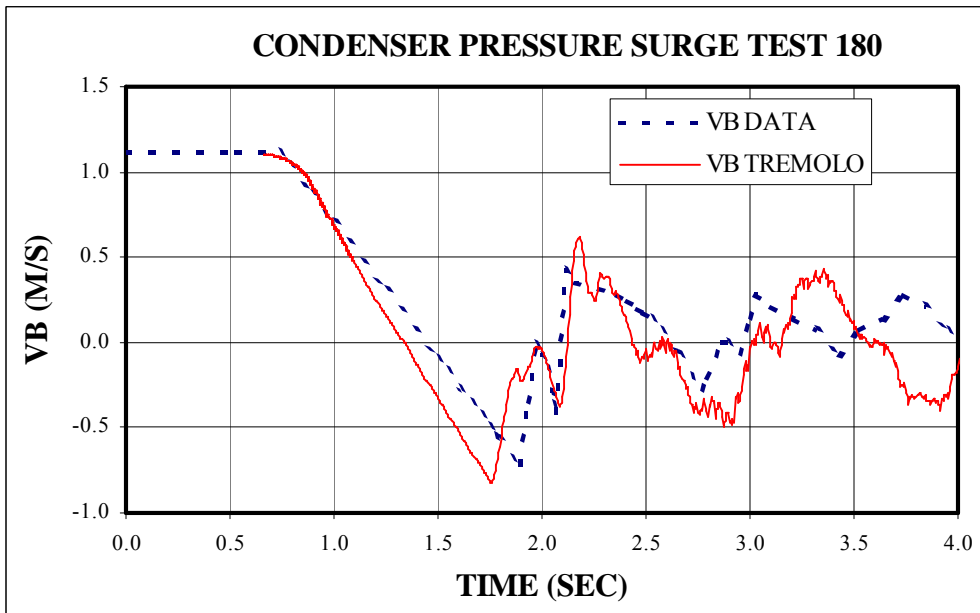
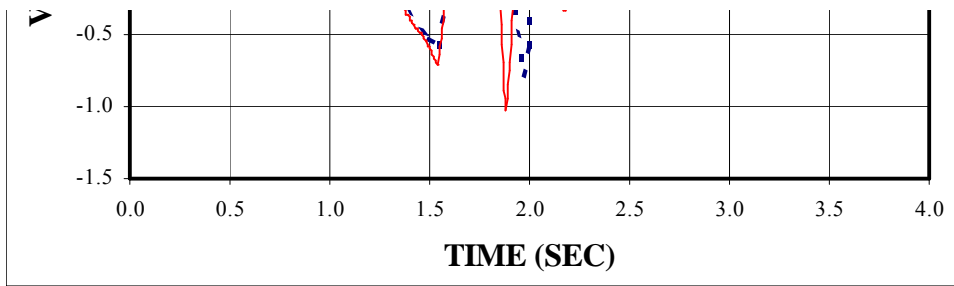


FIGURE 4 Test 180 Fluid Velocity Near Pipe Inlet (Instrument Position VA)

FIGURE 5 Test 180 Fluid Velocity Near Low Level Reservoir (Instrument Position VB)

Results for pressure surge test 180 are presented in Figures 4 through 7. The figures compare TREMOLO calculations and test data for the upstream fluid velocity, VA, the downstream fluid velocity, VB, system pressure, P1, and condenser outlet pressure, P7. The instrument locations for the VA, VB, P1, and P7 measurements are indicated in Figure 3. Figures 8 and 9 provide the TREMOLO-calculated axial void and flow profiles to demonstrate the behavior of the two separate water columns and void regions.

The TREMOLO calculation is started at 0.526 seconds -- once a significant resistance develops across the closing ball valve. While the apparatus for Test 180 used a ball valve, which is characterized by a flow coefficient that follows an s-shaped curve as a function of valve position, the TREMOLO valve model is designed to model a gate valve. The flow coefficient of a gate valve varies approximately as the square of the valve position. Thus, to approximate the Test 180 ball valve performance, the upstream boundary condition is modeled by simultaneously ramping down the upstream boundary pressure and closing a motor-operated valve (located in the first fluid node) such that

the P1 pressure profile and VA, through time of 0.894 seconds, is closely matched by TREMOLO. Beyond 0.894 seconds, the motor-operated valve is fully closed and the upstream boundary is isolated from the remainder of the test apparatus. Thus, for times greater than 0.894 seconds, the TREMOLO calculations of P1 and VA are based solely on the TREMOLO-calculated propagation of pressure waves through the single and two-phase portions of the fluid. Although data for test 180 is provided out to 8 seconds, the benchmark exercise is terminated at 4.0 seconds. Beyond 4 seconds, the fluid is essentially stagnant and no significant condensation-induced waterhammer events are observed.

As the result of three distinct waterhammer events between 1.5 and 2.25 seconds, three significant pressure rises are observed at location P1, shown in Figure 6, and two pressure rises are observed at location P7, shown in Figure 7. The first waterhammer event is caused by trapped void collapse near the closed ball valve as the water column supplying the condenser reverses direction due to gravity effects and impacts the closed valve. This is evidenced by the pressure rise at P1 (see Figure 6) and the sudden flow reversal exhibited at VA (see Figure 4) at 1.5 seconds.

During the next two waterhammer events, the supply side is essentially water solid from the valve up to the condenser (see Figure 8). The waterhammer events are initiated by column rejoining in the condenser region and propagation of the pressure waves through the upstream water column back to the closed valve. Figure 9 compares the TREMOLO-calculated velocities of the upstream and downstream water columns. At the instant of the first calculated void collapse in the condenser at 1.75 seconds, the water columns are approaching each other with calculated velocities at local maximum values of +0.35 m/s in the upstream column and -0.77 m/s in the downstream column. The experimental data exhibits the same behavior starting slightly later in time at 1.8 seconds. Data from Test 180 indicate that the water columns are approaching each other at a lower relative velocity than that calculated by TREMOLO, hence it is no surprise that the resulting waterhammer pressure rise calculated by TREMOLO at location P7 exceeds that observed in the test (see Figure 7).

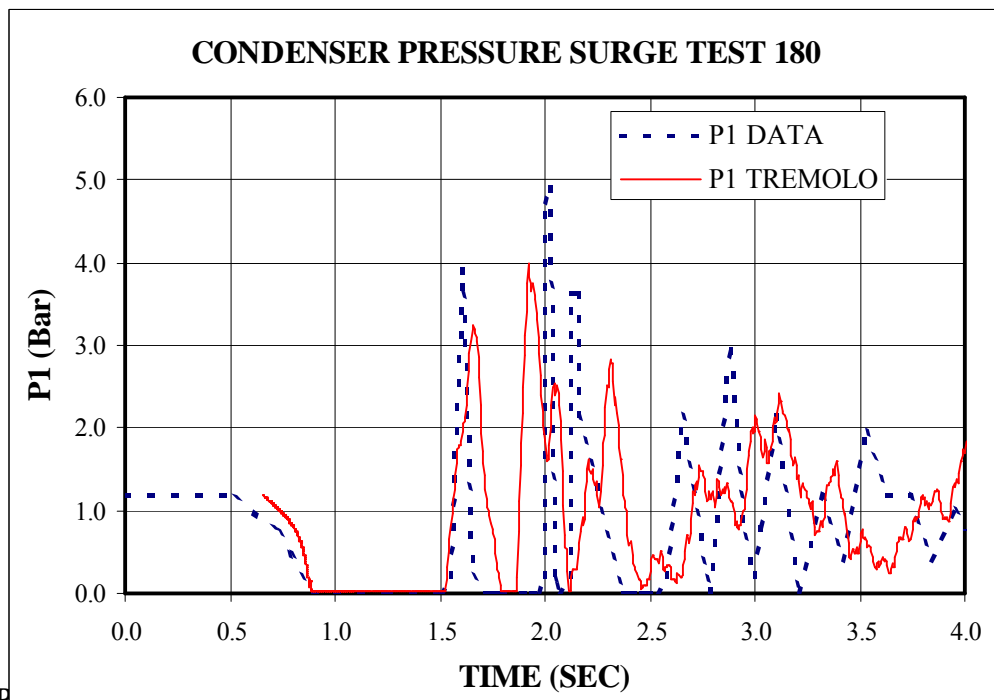


FIGURE 6. Test 180 Pressure from the Closed Valve (Benchmark Exercise 1)

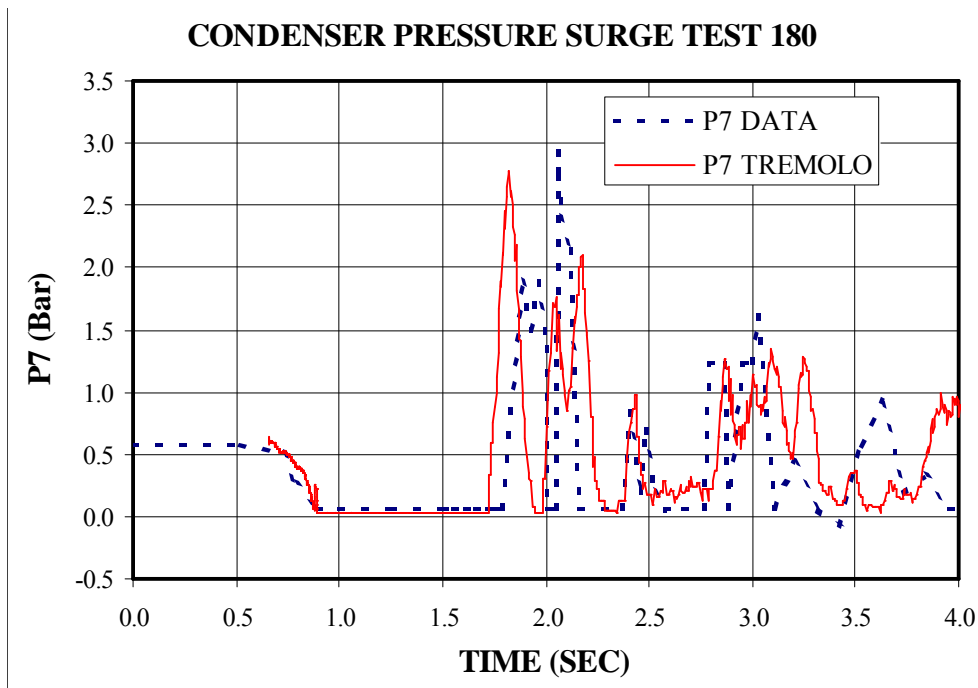


FIGURE 7 Test 180 Condenser Outlet Pressure (Instrument Position P7)

As the pressure wave originating in the condenser region at 1.75 seconds reaches the closed ball valve, a pressure increase at P1 occurs. In Figure 6, the TREMOLO calculations indicate the second P1 pressure rise at 1.8 seconds while the Test 180 data indicates the pressure rise occurs at about 1.95 seconds. The second waterhammer event indicated by P1 is larger in both the calculated and observed data than the first waterhammer pressure rise observed at P1. This is expected since the upstream water column velocity, V_A , at the time of the second waterhammer event is larger in magnitude than the velocity during the first waterhammer event (see V_A in Figure 4).

During the second column rejoining event in the condenser, calculated by TREMOLO at 2.0 seconds and observed experimentally at 2.1 seconds (see Figure 7), the water columns are approaching each other at calculated and observed relative velocities of 0.25 and 0.20 m/s, respectively (upstream column velocity calculated/observed: +0.25/+0.20 m/s, downstream column velocity calculated/observed: 0./0. m/s). This water column relative velocity is smaller than the relative velocity during the first column rejoining event in both the TREMOLO calculation and Test 180 data. However, the Test 180 data indicates a larger waterhammer pressure rise at P7 as compared to the pressure rise resulting from the first column rejoining event, whereas the TREMOLO calculations show a smaller pressure rise at P7 during the second column rejoining. This is possibly due to the influence of the

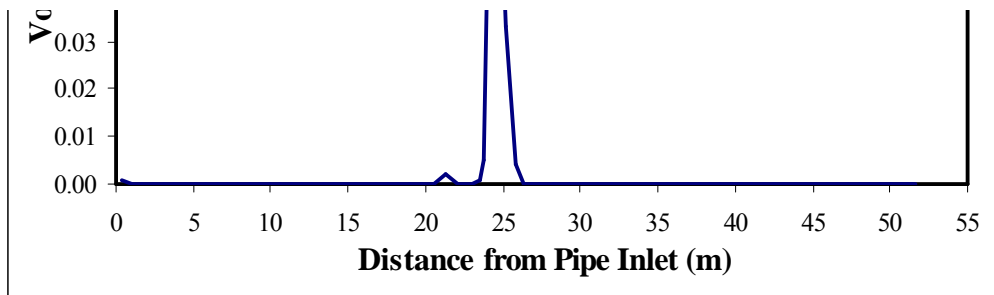


FIGURE 8 Test 180 TREMOLO-Calculated Axial Void Profile Prior to Column Rejoining in the Condenser (Condenser is located from 22 to 27 m from the pipe inlet)

residual void on the waterhammer event. Additionally, the Test 180 data indicates a faster wave transmission time between P7 and P1 than that calculated in TREMOLO, as inferred from the difference in timing of the P7 and P1 pressure rises. The faster wave transmission time and larger pressure rise in the Test 180 data both indicate a smaller influence of the voids during the second column rejoining event than that credited in TREMOLO.

Although the three significant condensation-induced waterhammer events discussed previously are present in the Test 180 data and the TREMOLO calculations, the experimentally observed timing of the events and the resulting pressure rises are not precisely predicted by TREMOLO. This is primarily the result of two factors. First, it is difficult to match the upstream boundary condition because the influence of the high-level reservoir was controlled experimentally by closing a ball valve, while the TREMOLO valve model is designed to match gate valve closure. Second, the residual void model in TREMOLO only approximates the actual behavior of the non-condensable gases.

Despite the differences between the actual test configuration and the TREMOLO modeling capabilities, the benchmark does demonstrate the ability of TREMOLO to model the essential aspects of cold water column separation postulated to occur during loss of power events at nuclear power plants. Namely, this benchmark exercise indicates that the TREMOLO Revision 1 models can adequately model column separation and rejoining, fluid flow reversals, the behavior of multiple voided regions, the movement of multiple water columns, and the transmission of pressure waves through a combined single and two-phase fluid.

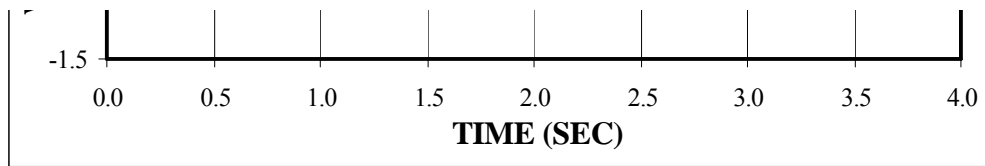


FIGURE 9 Test 180 Water Column Velocities Calculated by TREMOLO

5.0 CONCLUSIONS

The TREMOLO dynamic benchmarking effort has demonstrated the code's ability to analyze column separation and condensation-induced waterhammer events that could occur in the cooling water piping systems of nuclear power plants. In particular, the benchmarking activities demonstrated the code capability to adequately model key phenomena encountered in transient waterhammer and two-phase flow analyses, such as,

- Sonic velocity in single and two-phase mixtures
- Column separation and rejoining
- Pressure wave transmission in combined single and two-phase fluids
- Movement of multiple water columns
- Void collapse in multiple voided regions
- Fluid flow reversal

Furthermore, the dynamic benchmarking exercises validate the TREMOLO approach of using a one-dimensional, five equation fluid model with assumptions of residual void to analyze the types of transient thermal hydraulic events postulated to occur in the service water piping systems of nuclear power plants.

NOMENCLATURE

a_w	sonic velocity in the fluid
c_p	specific heat at constant pressure
f	friction factor
h	heat transfer coefficient
K	numerical damping factor
P	pressure
T	absolute temperature
u	fluid velocity
w	mass flow rate
Δt	time step
Δx	node length
ρ	fluid density

Subscripts

b bulk
fluid fluid mixture property
i node i
i-1 node i-1
i+1 node i+1
max maximum limit
sat saturation property at the water temperature

ACKNOWLEDGMENTS

The efforts of many individuals went into the development of the TREMOLO computer code and should not be overlooked. Specifically, Steve Dawson developed several of the dynamic benchmark subroutines, Dr. Hugh Campbell spent many hours with the code during its initial development to address Generic Letter 89-10 issues, George Hauser provided the water properties routines and has spent numerous hours debugging the code, and finally Boro Malinovic has provided many ideas and papers on code numerics and benchmarking that have been instrumental in the TREMOLO code development.

REFERENCES

- Cerne, G., Tiselj, I., Petelin, S. (Jozef Stefan Inst., Slovenia), 1996. Modeling of Water Hammer with Column Separation. *Transactions of the American Nuclear Society*, 387-388.
- Hammersley, R. J., Elicson, G. T., Henry, R. E., 1999, Two-Phase Flow and Waterhammer Transient Assessments with the TREMOLO Computer Code. To be published in the *Trans. ASME*.
- Henry, R. E., Paik, C. Y., Hauser, G. M., 1996a. MAAP4 Dynamic Benchmarking. *Trans. ANS Summer Meeting*, **74**, 362.
- Henry, R. E., Paik, C. Y., and Hauser, G. M., 1996b. Dynamic Benchmarking of Simulation Codes. Paper presented at the *Fifth International Conference on Simulation Methods and Nuclear Engineering*, Montreal, Canada (September, 1996).
- Henry, R. E., Paik, C. Y., Hauser, G. M., 1997a. Dynamic Benchmarking of Simulation Codes. *Transactions of the 1997 ANS Summer Meeting*.
- Henry, R. E., Paik, C. Y., Schlenger-Faber, B., Henry, C. E., McCartney, M. A., Fauske & Associates, Inc, and Chao, J., Electric Power Research Institute, 1997b. Dynamic Benchmarking Program for the MAAP4 Code. NUREG/CP-0162 *Proc. of the U. S. Nuclear Regulatory Commission 25th Water Reactor Safety Information Meeting, Bethesda, MD*, **1**.
- Henry, R. E., 1999. Waterhammer in Horizontal Lines During the Voiding Phase. To be published in the *NURETH-9 Proceedings*.
- Holman, J. P., 1981. *Heat Transfer*, McGraw-Hill Book Company, New York, pp. 195.
- Izenson, M. G., Rothe, P. H. and Wallis, G. B., 1988. Diagnosis of Condensation-Induced Water Hammer. NUREG/CR-5220, Creare TM-1189, Volumes 1 and 2.
- Paik, C. Y., McCartney, M. A., Henry, R. E., 1996. Validation Exercise for the MAAP4 Containment Model. Paper presented at the *Fifth International Conference on Simulation Methods and Nuclear*

Engineering, Montreal, Canada (September, 1996).

Safwat, H. H., Delft University of Technology, The Netherlands, 1972. Experimental Study of Pressure Surges in Condenser Cooling Water Systems. *Proceedings of the 1st International Conference on Pressure Surges*, Canterbury, England, pp. D2-17 – D2-32 (September 6-8, 1972).

Serkiz, A. W., 1984. Evaluation of Water Hammer Occurrence in Nuclear Power Plants. Technical Findings Relevant to Unresolved Safety Issue A-1, NUREG-0927, Rev. 1.

Tong, L. S., 1965. *Boiling Heat Transfer in Two-Phase Flow*, John Wiley & Sons Incorporated, New York, London and Sydney.

USNRC, 1979. Waterhammer in Nuclear Power Plants. NUREG-0582.

USNRC, 1989, Generic Letter 89-10: Safety-Related Motor-Operated Valve Testing and Surveillance.

USNRC, 1996, Generic Letter 96-06: Assurance of Equipment Operability and Containment Integrity During Design Basis Accident Conditions.

Wylie, E. B. and Streeter, V. L., 1978. *Fluid Transients*, McGraw-Hill Book Company, New York, pp. 39.